ENGINEERING RESEARCH JOURNAL (ERJ)
Vol. 1, No. 40 April 2019, pp.16-23.
Journal Homepage: www.feng.bu.edu.eg

Hardness and Wear Behaviour Of Al_2O_3/AA6063 Surface Metal Matrix Composites Fabricated Using Friction Stir Processing

B.H. ElSayed[1] E.H. Mansour[2] T.S. Mahmoud[2] T.A. Khalifa[2]

[1]Egyptian Academy for Engineering & Advanced Technology (EAE&AT) affiliated to ministry of military production, Cairo, Egypt.

[2] Mechanical Engineering Department, Faculty of Engineering at Shoubra , Benha university.

ABSTRACT

The hardness and wear characteristics of Al_2O_3/AA6063 aluminum surface composites (SCs) fabricated by Friction Stir Processing (FSP) were evaluated. The FSP process parameters effect, typically, the tool rotational and traverse speeds on the aforementioned characteristics were studied. It has been found that the Al_2O_3/AA6063 composite layers have higher microhardness values when compared with the AA6063 base alloy. By increasing both the tool rotational and traverse speeds and one of them, increases(s) the microhardness of the Al_2O_3/AA6063 composite layers. The wear resistances of the Al_2O_3/AA6063 composite layers increases with increasing the tool rotational speed and/or reducing the tool traverse speed.

KEYWORDS: Friction Stir Processing, Wear, Hardness, Surface Composites, Aluminum Alloys.

1. INTRODUCTION

Surface composites of Metal matrix, is a new class of metal matrix composites (MMCs) [1]. They can overcome the defects of general bulk MMCs such as low toughness and ductility [2]. MMSCs are produced by saturating the particulates of the surface only without saturating the core. The MMSCs may be used in machine parts subjected to wear such as cams, gears, pistons and more other applications where a good tribological behaviors with more relative strength and toughness are desirable [1,2]. MMSCs with adequate strength at low cost were successfully produced using several techniques such as laser treatment, ultrasonic treatment and friction stir processing (FSP) [1-4]. The latest is one of the most economical routes for fabricating such composites. Over the last period, FSP attracted interest when its first trial towards the fabrication of MMSCs by FSP that reported via *Mishra et al.* [5]. FSP is considered a relatively new technique of processing that was developed to modify the microstructural and based on the principle of friction stir welding (FSW). By the same way of FSW, The FSP is carried out also by immersing a rotating tool in to the workpiece. The generated heat from the friction between the work piece and tool softens the material, however the work piece never melts, and a bulk of the substance can then be processed while the tool go forward. The MMCs fabrication and by FSP is valuable because the unwanted particles/matrix interfacial reactions and intermetallic materials which can be formed between enforcement and matrix can be canceled [1, 2, 5].

The aim of the present investigation is to fabricate micro-Al_2O_3/AA6063 Al SCs using FSP. Several FSP tool rotation and traverse speeds were applied to raise material mixing, creating a uniform dispersal of particles. The effects of micro-Al_2O_3 particles addition as well as the FSP aforementioned parameters on microstructure, hardness and wear resistance of the friction stir (FS) processed AA6063 Al matrix were investigated.

2. EXPERIMENTAL PROCEDURES

The AA6063 (Al-Zn-Mg-Si) Al wrought alloy was used as a matrix material. The chemical composition of the AA6063 alloy is listed in Table 1. The material was received in the form of large rolled plates and cut perpendicularly to the rolling direction. FSP specimens having dimensions of [100 mm (length) × 20 mm (width) × 10 mm (thickness)] with a groove dimension of [80 mm (length) × 2 mm (width) × 2 mm (depth)] were cut longitudinally along the rolling direction of the as-received plates. Figure 1 shows a schematic drawing of the FSP specimens. Aluminum oxide (Al_2O_3) micro-size ceramic particulates were used as a reinforcement. The Al_2O_3 particulates have a size range varies between 0.5 and 4 µm with an average size of 2.5 µm.

Alloy	Chemical compositions (wt.%)								
	Si	Fe	Cu	Mg	Mn	Ni	Zn	Ti	Al
AA6063	0.4	0.35	0.1	0.67	0.5	0.35	0.1	0.25	Bal.

Table 1. Chemical composition of AA6063 alloy.

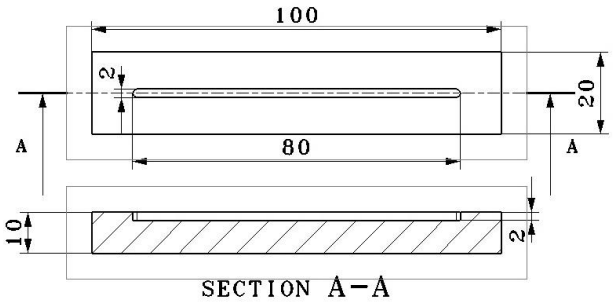

Fig. 1. A schematic drawing of the FSP specimens (dimensions in mm).

The Al_2O_3/AA6063 SCs were fabricated using FSP in two passes using two different steel tools shown schematically in Fig. 2. The first FSP tool is a pinless tool and it has a shoulder diameter of 18 mm as shown in Fig. 2a. The second FSP tool has a pin of 7 mm diameter and a height of 4mm, and a shoulder with diameter 18 mm (see Fig. 2b). This pin was plunged into the workpiece and traveled along the closed groove. Both FSP tools are made from H13 tool steel. The chemical composition of the H13 tool steel is listed in Table 2.

Table 2. Chemical composition of H13 steel.

Alloy	Chemical Composition wt. %						
	C	Mn	Cr	V	Mo	Si	Fe
H13	0.39	0.40	5.2	0.95	1.4	1.10	Bal.

The first step was cleaning the surface of AA6063 alloy plates before processing. Then the aluminum oxide particulates were added with small amount of methanol and they were mixed together, and then they were applied to the plate from its surface in the groove to create thin reinforced aluminum oxide particulates layer. A vertical milling machine was used to conduct the FSP by three different rotational speeds of the tool , respectively, 560, 710 and 900 rpm and three feed rates (traverse speeds), typically, 16, 20 and 25 mm/min. In the entire experiments, the groove was closed after filling by using the pinless tool with rotational speed (560 rpm) and traverse speed (16 mm/min). During FSP, the tool having a pin was operated with a fixed tool angle of 2º and the tool downforce was held constant. Figure 3 shows a schematic illustration of the FSP carried out in the present investigation.

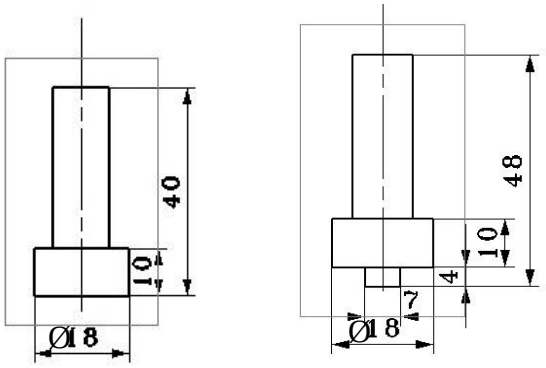

(a) (b)

Fig. 2. Schematic illustration of the FSP tools (Dimensions in millimeters).

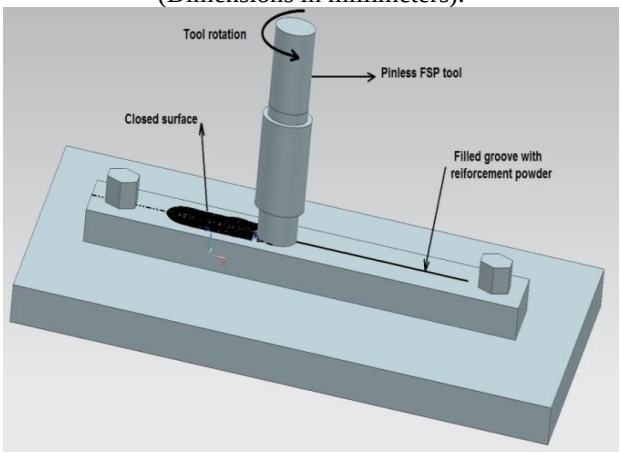

(a)

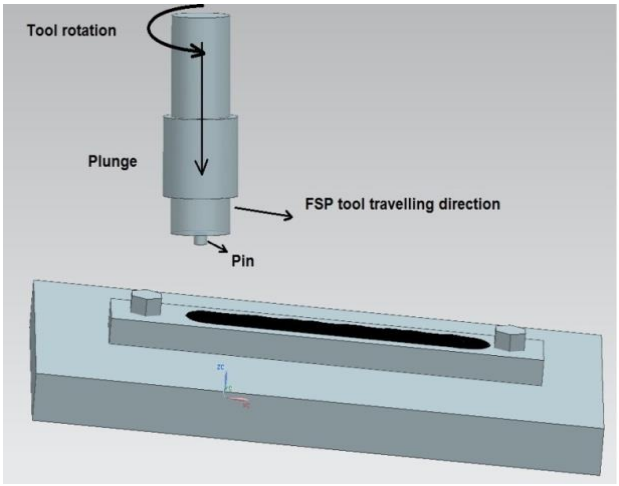

(b)

Fig. 3. Schematic illustration of SCs fabrication process. (a) Step 1: closing the filled groove using the FSP pinless tool, (b) Step 2: FSP of the Al_2O_3/AA6063 layer using a tool with a pin.

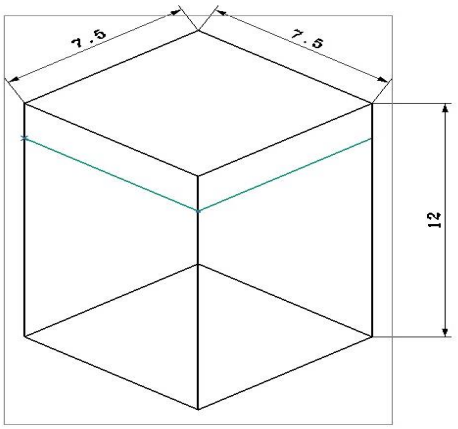

(Dimensions in millimeters)
(a)

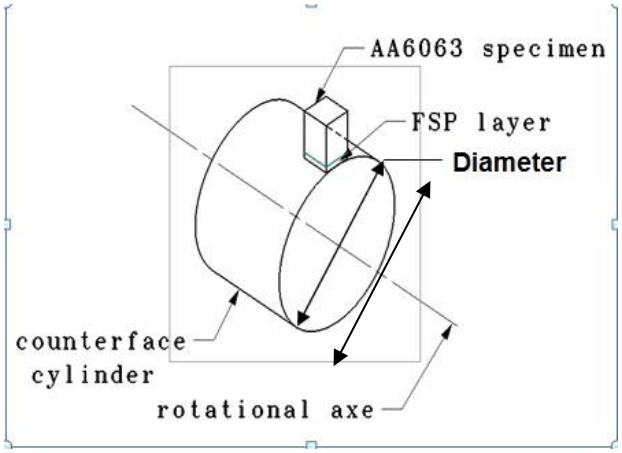

(b)

Fig. 4. Schematic illustration of (a) the wear specimens and (b) the wear test.

3. RESULTS AND DISCUSSION

3.1. Macro- and Microstructural Investigations

Figure 5 shows typical sample macrographs of the Al_2O_3/AA6063 SCs specimens. The Al_2O_3/AA6063 friction stir (FS) processed region is indicated in the figure. It is important to mention that all the Al_2O_3/AA6063 SC samples were free from defect such as large cavities and tunnel defects. There was obvious difference between the Al_2O_3/AA6063 SC zones and the base metal. The Al_2O_3/AA6063 SC zones were easily identified. The microstructure of the FSP is often formed from four essential zones: the first one is base metal (BM), secondly the heat-affected zone (HAZ), thirdly the thermo-mechanically affected zone (TMAZ), and finally the stirred zone (SZ). Figure 5 shows clearly the SZ in the SCs specimens.

Figure 6 shows optical micrograph of the microstructure of the as-received AA6063 matrix alloy. The microstructure of the as-received AA6063 matrix alloy exhibited large elongated grains typical of a rolled structure, with an average grain size of 210 μm and an aspect ratio of ~7.2. The grains in the base alloy have an orientation along the rolling direction. Figure 7 shows optical micrographs of the microstructure of the developed SCs friction stir processed at different tool rotational and traverse speeds. The micrographs were taken at the center of the stirred zones of the FS processed regions. The micrographs indicate the effectiveness of the FSP technique in fabricating Al_2O_3/AA6063 SCs. It is clear that the Al_2O_3 particles are fairly distributed inside the SC layer. Figure 8 shows example SEM micrograph of Al_2O_3/AA6063 SC layer. The figure shows an example of EDX analysis of Al_2O_3 particulates shown in the SEM micrograph. It has been observed that the Al_2O_3 particulates were fragmented, at higher tool rotational speeds due to collision with the rotational pin or other particles. In addition, it can be seen that the reinforcements are distributed in refined grain substrate. In the Al_2O_3/AA6063 SCs layers, the primary α-Al grains are equiaxed and the microstructure is relatively fine as compared to the microstructure of the AA6063 as-received alloy. This is due to that the material while the FSP practiced strong stirring and mixing, which lead to breaking up of the coarse α-Al grains and gave fine and equiaxed α-Al grains. Figure 9 shows the variation of the average grain size of the α-Al grains with the tool traverse speed at several tool rotational speeds. The results revealed that increasing the tool rotational speed reduces the average grain size of the α-Al grains perhaps due to the increase of nucleation rate as a result of broken small sized Al_2O_3 particulates. Figure 9 shows also that, at constant tool rotational speed, increasing the tool traverse speed slightly reduces the average size of the α-Al grains.

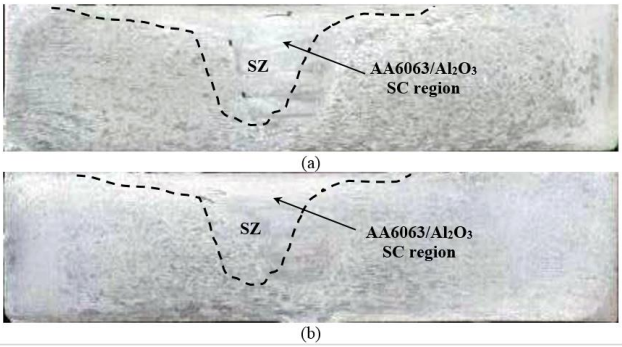

Fig. 5. Macrostructure for FS processed Al_2O_3/AA6063 SCs specimens. The FSP was carried out at tool rotational of 560 rpm and traverse speed of (a) 16 mm/min and (b) 20 mm/min, respectively.

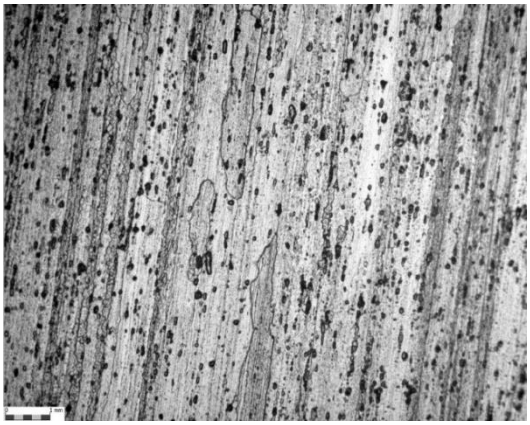

Fig. 6. Optical micrograph for
the microstructure of AA6063 as-received matrix alloy.
The arrow indicates the rolling direction.

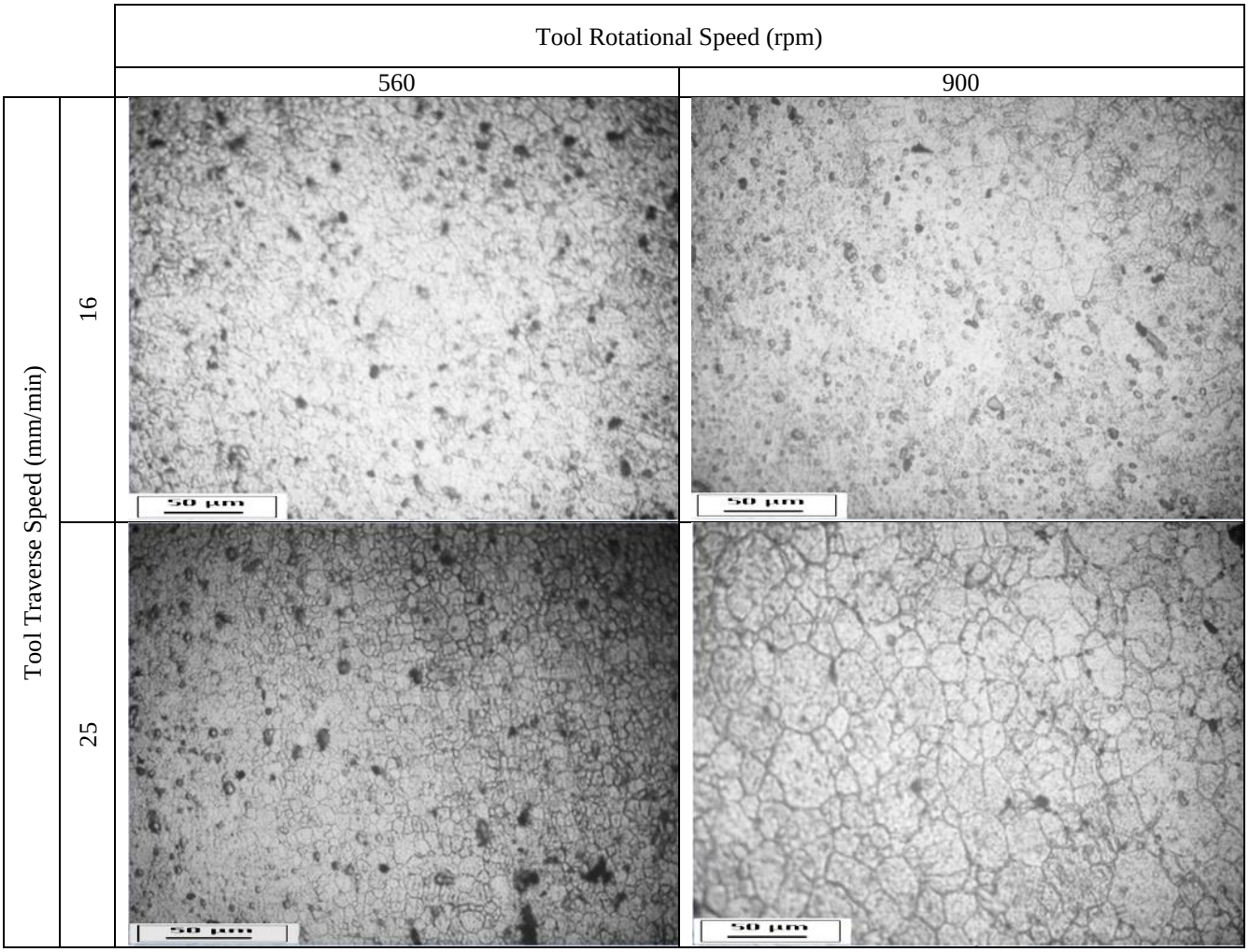

Fig. 7. Micrographs for the microstructure on optical microscope of the SCs FS processed at different tool rotational and traverse speeds.

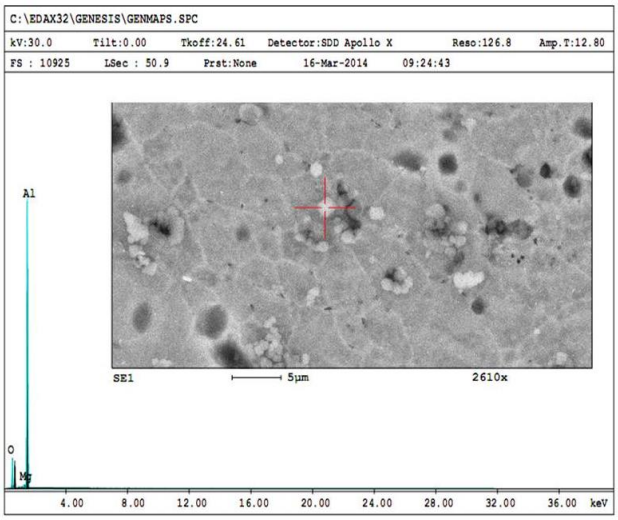

Fig. 8. SEM micrograph of Al_2O_3/AA6063 SCs specimens and EDX analysis of a particle indicating that the particles chemical composition is Al_2O_3.

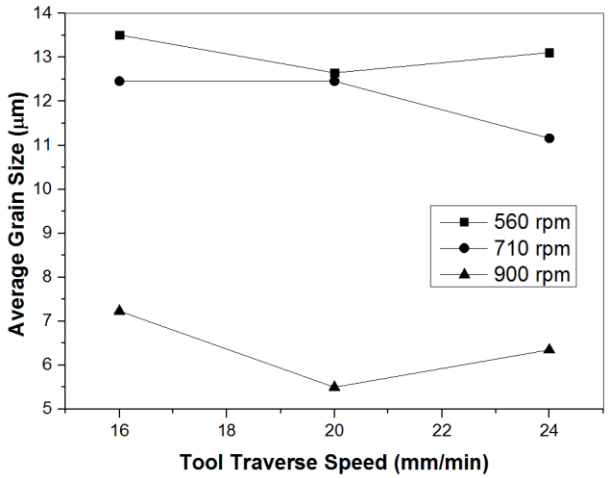

Fig. 9. Variation of α-Al grains average size, at the center of Al_2O_3/AA6063 SCs areas, with the tool traverse speed with the different rotational speeds.

The variation of the Al_2O_3 particles volume fraction by the traverse speed at several angular speeds are illustrated in Fig. 10. Agglomeration of particles was observed in the FS processed layer. It has been found that some of Al_2O_3 particulates were separated uniformly into the AA6061 alloy matrix; on the other hand, the others were conglomerated. It is found that the particulates were cracked due to the strong stirring action through FSP.

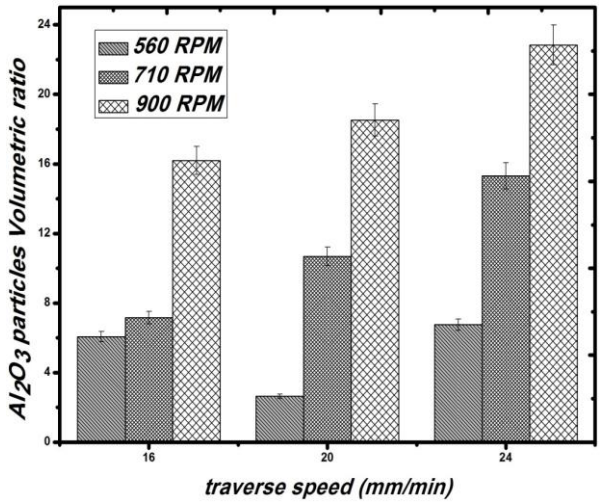

Fig. 10. Variation of the average Al_2O_3 particles volume fraction, in the Al_2O_3/AA6063 FS processed regions, with the tool traverse speed at different rotational speeds.

3.2. Micro-Hardness.

Figure 11 shows the deference of the average micro-hardness of the Al_2O_3/AA6063 SC layer with the tool rotational speed at different travel speeds. The AA6063 base alloy presented average micro-hardness of 107 VHN. The Al_2O_3/AA6063 SC layers presented higher micro-hardness comparing to the AA6063 matrix alloy.

The results revealed that the microhardness of the Al_2O_3/AA6063 SC layers based on the FSP processing variables, respectively, the travelling and rotational speeds. At one travelling speed, while increasing of the rotational speed, the average microhardness of the Al_2O_3/AA6063 SC layer increases. Moreover, at constant tool rotational speed, increasing the traverse speed increases the average microhardness of the Al_2O_3/AA6063 SC layer. While, the maximum average microhardness of the Al_2O_3/AA6063 SC is about 193 VHN for Al_2O_3/AA6063 SC layer FS processed at travelling tool and rotational speeds of 900 rpm and 24 mm/min, respectively. This presents increasing in the hardness of about 55% compared with the AA6063 base metal hardness.

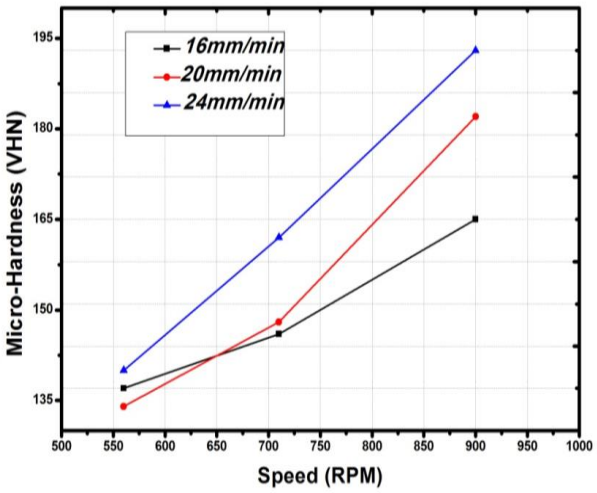

Fig. 11. The variation of microhardness of the Al_2O_3/AA6063 SC layers with rotational speed at different travelling speeds.

The enhancement of the mean hardness of the Al_2O_3/AA6063 SC layers in comparison with the AA6063 matrix alloy may attribute to two factors: (1) the dispersion of the hard Al_2O_3 particles inside the AA6063 matrix and (2) microstructural development because of FSP such as the grain refinement of the AA6063 base alloy. In this investigation, increasing the tool rotational speed and/or the tool traverse speed resulted in a reduction of the size of the recrystallized α-Al grains and hence increases the hardness of Al_2O_3/AA6063 SC layers. The enhancement of the hardness with grain refinement of the α-Al phase may be explained using *Hall-Petch* equation [6]. The relationship between the hardness (H_v) and the grain size (d) can be explained using the following Hall–Petch equation [6]:-

$$H_v = H_0 + k_H \cdot d^{-1/2} \quad \ldots(1)$$

Where H_0 and k_H are appropriate constants. It is clear from Eq. (1) that H_v is proportional to $d^{-1/2}$. According to the above equation, the finer the grain size is, the higher the hardness value is. The improvement of the hardness due to the dispersion of ceramic particulates for Al and Mg based composites fabricated using FSP was reported by many workers [1, 5, 7].

3.3. Wear Behavior of Al_2O_3/AA6063 Surface Composites

Figure 12 shows the different of the rate of wear of Al_2O_3/AA6063 SCs specimens with the angular speed at different traverse speeds. It has been found that, when the traverse speed is constant, the increasing of the rotational speed decreases the wear rate of the SCs specimens. For example, at constant traverse speed of 20 mm/min, increasing the tool rotational speed from 560 to 900 rpm reduced the wear rates of Al_2O_3/AA6063 SC specimens from 5.38×10^{-6} to 3.57×10^{-6} g/sec, respectively. Moreover, when the angular speed is constant, the increasing of the travelling speed growing the wear rate of Al_2O_3/AA6063 SC specimens.

Figures 13 show typical SEM micrographs of the worn surfaces of the surface composites FS processed at constant tool rotational speed of 900 rpm and traverse speeds of 16 mm/min and 20 mm/min, respectively. It can be seen that the worn surface of the sample FS processed at 16 mm/min exhibited smoother worn surface than that of sample FS processed at 20 mm/min. For the sample FS processed at 16 mm/min, only slight plough and scratch marks were observed on the worn surface (See Fig. 13a). In the case of SCs FS processed at 20 mm/min the number of ploughs and scratches were increased (see Fig. 3.21). Figure 14 shows SEM micrograph of the worn surface of a sample FS processed at travelling an d angulat speeds of 710 rpm and 20 mm/min. Comparing Fig. 13 and Fig. 14, it is clear that of the sample shown in Fig. 3.22 (i.e. FS processed at 710 rpm) has smoother worn surface than that shown in Fig. 13 (i.e. FS processed at 900 rpm).

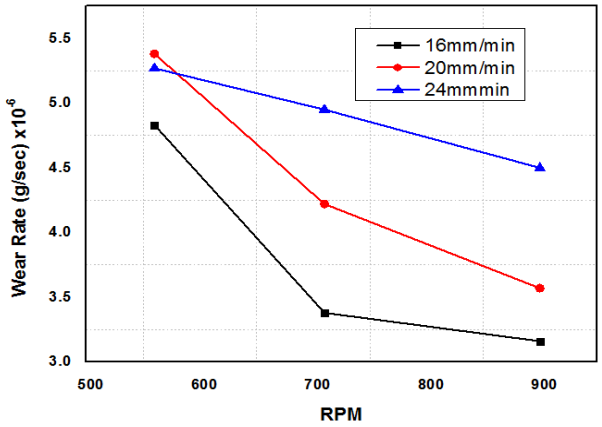

Fig. 12. The variation of the wear rate of the Al_2O_3/AA6063 SC specimens with the angular speed at different tool travelling speeds.

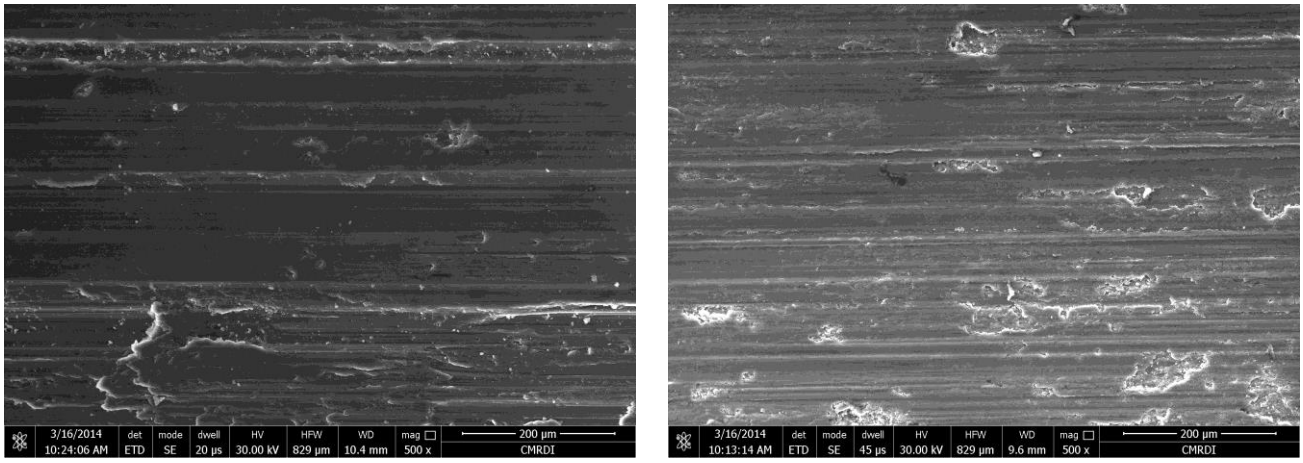

(a) (b)

Fig. 13. SEM micrographs of the worn surfaces of the SCs FS processed at constant tool rotational speed of 900 rpm and traverse speeds of 16 mm/min (a) and 20 mm/min (b).

The SCs exhibited classical features of the dry sliding wear. It is clear from the SEM micrographs that abrasive wear is considered the essential wear technique. Such technique mainly comes due to the hard ceramic particles uncovered on the worn surface and the fractions between the two surfaces, controls in layers of SCs. The relatively low wear rates exist, pointing the regime of mild wear.

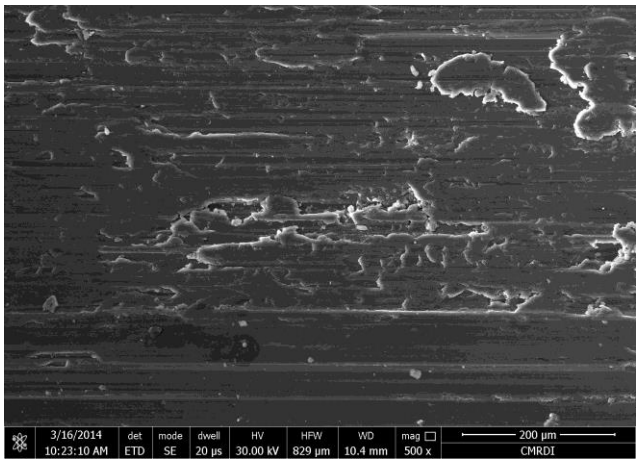

Fig. 14. Micrographs of SEM test of the worn surfaces of specimens FS processed at 20 mm/min and 710 rpm.

4. CONCLUSIONS

Owing to the obtained results of this work, these conclusions are drawn:

1 - The surface composite layers exhibited a very fine grain structure. The surface composite layers have an average grain size range of α-Al primary phase between ≈ 5.5 and ≈13.5 µm. At constant travelling speed, increasing the tool angular speed significantly reduces the size of the α-Al primary phase grains. The travelling speed slight significant influence of the average size of the α-Al grains. The minimum α-Al primary phase grain size of about ≈ 5.5 µm was observed for sample FS processed using tool angular and travelling speeds of 900 rpm and 20 mm/min, respectively.

2 - The Al_2O_3/AA6063 SCs exhibited higher microhardness values than the AA6061 monolithic base alloy. Increasing the tool angular speed and/or the travelling speed increase(s) the microhardness of the Al_2O_3/AA6063 surface composite layers. The maximum average microhardness of the Al_2O_3/AA6063 SC was ≈193 VHN for surface composite layer FS processed using tool angular and travelling speeds of 900 rpm and 24 mm/min, respectively.

3 - The dry sliding wear resistance of the Al_2O_3/AA6063 SCs layers was found to increase by increasing the tool angular speed and/or reducing the tool travelling speed. The minimum wear rate was observed for a sample FS processed using tool angular and travelling speeds of 900 rpm and 16 mm/min, respectively.

ACKNOWLEDGMENTS

The authors are thankful to the Egyptian Academy for Engineering & Advanced Technology, Benha University and Science, and Technology Center of Excellence for providing financial and technical support for carrying out this study.

REFERENCES

[1] Rajiv Singh and James Fitz-Gerald, "Surface composites: A new class of engineered materials", Journal of Materials Research, 12(3), 1997, pp. 769-773.

[2] Y. Mazaheri, F. Karimzadeh, M.H. Enayati, "A novel technique for development of A356/Al_2O_3 surface nanocomposite by friction stir processing", Journal of Materials Processing Technology, 211, 2011, pp. 1614–1619.

[3] M. Li, Y. He, X. Yuan, Sh. Zhang, "Microstructure of Al_2O_3 nanocrystalline/cobalt-based alloy composite coatings by laser deposition", Materials and Design, 27, 2006, pp. 1114–1119.

[4] S. Yu, H. Feng, Y. Li, "A novel method for preparing Al matrix surface composites", Journal of Alloys and Compounds, 457, 2008, pp. 404–407.

[5] R.S. Mishra, Z.Y. Ma, I. Charit, "Friction stir processing: a novel technique for fabrication of surface composite", Materials Science and Engineering A, A341, 2003, pp. 307–310.

[6] Park, Seung Hwan C., Sato, Yutaka S., Kokawa Hiroyuki, "Microstructural evolution and its effect on Hall-Petch relationship in friction stir welding of thixomolded Mg alloy AZ91D", Journal of Materials Science, 38(21), 2003, pp. 4379-4383.

[7] M. Raaft, T.S. Mahmoud, , H.M. Zakaria, T.A. Khalifa, " Microstructural, mechanical and wear behavior of A390/graphite and A390/Al_2O_3 surface composites fabricated using FSP", Materials Science and Engineering A, 528 (18), 2011, pp. 5741–5746.